

# The cholesterol transporter ABCG1 modulates the subcellular distribution and proteolytic processing of $\beta$ -amyloid precursor protein

Gavin H. Tansley,<sup>1,\*</sup> Braydon L. Burgess,<sup>1,\*</sup> Matt T. Bryan,<sup>†</sup> Yuan Su,<sup>†</sup> Veronica Hirsch-Reinshagen,<sup>\*</sup> Jonathan Pearce,<sup>\*</sup> Jeniffer Y. Chan,<sup>\*</sup> Anna Wilkinson,<sup>\*</sup> Jeanette Evans,<sup>\*</sup> Kathryn E. Naus,<sup>\*</sup> Sean McIsaac,<sup>\*</sup> Kelley Bromley,<sup>§</sup> Weihong Song,<sup>§</sup> Hsui-Chiung Yang,<sup>†</sup> Nan Wang,<sup>\*\*</sup> Ronald B. DeMattos,<sup>†</sup> and Cheryl L. Wellington<sup>2,\*</sup>

Department of Pathology and Laboratory Medicine,<sup>\*</sup> University of British Columbia, Vancouver, British Columbia, Canada; Lilly Research Laboratories,<sup>†</sup> Indianapolis, IN; Department of Psychiatry,<sup>§</sup> Brain Research Centre, University of British Columbia, Vancouver, British Columbia, Canada; and Department of Medicine,<sup>\*\*</sup> Columbia University, New York, NY

**Abstract** Although intracellular cholesterol levels are known to influence the proteolysis of  $\beta$ -amyloid precursor protein (APP), the effect of specific genes that regulate cholesterol metabolism on APP processing remains poorly understood. The cholesterol transporter ABCG1 facilitates cholesterol efflux to HDL and is expressed in brain. Notably, the human ABCG1 gene maps to chromosome 21q22.3, and individuals with Down syndrome (DS) typically manifest with Alzheimer's disease (AD) neuropathology in their 30s. Here, we demonstrate that expression of ABCG1 enhances amyloid- $\beta$  protein (A $\beta$ ) production in transfected HEK cells in a manner that requires functional cholesterol transporter activity. ABCG1-expressing cells also exhibit increased secreted APP (sAPP) $\alpha$  and sAPP $\beta$  secretion and display increased cell surface-associated APP. These results suggest that ABCG1 increases the availability of APP as a secretase substrate for both the amyloidogenic and nonamyloidogenic pathways. In vivo, ABCG1 mRNA levels are 2-fold more abundant in DS brain compared with age- and sex-matched normal controls. Finally, both A $\beta$  and sAPP $\alpha$  levels are increased in DS cortex relative to normal controls. These findings suggest that altered cholesterol metabolism and APP trafficking mediated by ABCG1 may contribute to the accelerated onset of AD neuropathology in DS.—Tansley, G. H., B. L. Burgess, M. T. Bryan, Y. Su, V. Hirsch-Reinshagen, J. Pearce, J. Y. Chan, A. Wilkinson, J. Evans, K. E. Naus, S. McIsaac, K. Bromley, W. Song, H-C. Yang, N. Wang, R. B. DeMattos, and C. L. Wellington. **The cholesterol transporter ABCG1 modulates the subcellular distribution and proteolytic processing of  $\beta$ -amyloid precursor protein.** *J. Lipid Res.* 2007. 48: 1022–1034.

**Supplementary key words** ATP binding cassette transporter G1 • Alzheimer's disease • amyloid  $\beta$  proteins • Down syndrome

Manuscript received 21 December 2006 and in revised form 1 February 2007.  
Published, JLR Papers in Press, February 10, 2007.  
DOI 10.1194/jlr.M600542-JLR200

One of the major neuropathological hallmarks of Alzheimer's disease (AD) is the accumulation of amyloid deposits in the brain parenchyma and within cerebral blood vessels (1). Amyloid plaques are composed mainly of fibrillar aggregates of amyloid- $\beta$  protein (A $\beta$ ) that are derived from  $\beta$ -amyloid precursor protein (APP) by proteolytic cleavage. Most APP molecules are cleaved by  $\alpha$ -secretase at a site within the A $\beta$  domain to release the neurotrophic ectodomain of APP, a process that precludes the generation of A $\beta$ . In contrast, cleavage of APP by  $\beta$ - and  $\gamma$ -secretases generates the A $\beta$  peptides found in amyloid plaques (2).

Cholesterol is increasingly recognized to play a key role in the pathogenesis of AD (3). Many groups have reported that high intracellular cholesterol levels result in enhanced release of A $\beta$  in vitro and in vivo (4–7), whereas low intracellular cholesterol levels favor processing of APP through the nonamyloidogenic  $\alpha$ -secretase pathway and decrease A $\beta$  production (8–13). Intracellular cholesterol also affects the subcellular distribution of presenilins (7, 14), and  $\beta$ -secretase cleavage of APP is dependent on the association of APP with BACE1 in lipid rafts (13). Notably, many of these studies have relied upon pharmacological or chemical manipulation of intracellular cholesterol levels to investigate the relationship between cholesterol and APP processing. However, physiological regulation of intracellular cholesterol levels is mediated by a network of genes involved in sterol homeostasis, and the specific effect of many of these genes on APP processing is not well understood.

Abbreviations: A $\beta$ , amyloid- $\beta$  protein; AD, Alzheimer's disease; apoA-I, apolipoprotein A-I; APP,  $\beta$ -amyloid precursor protein; CTF, C-terminal fragment; DS, Down syndrome; sAPP, secreted APP.

<sup>1</sup> G. H. Tansley and B. L. Burgess contributed equally to this work.

<sup>2</sup> To whom correspondence should be addressed.

e-mail: cheryl@cmmt.ubc.ca

ATP binding cassette transporters use ATP hydrolysis to drive the transport of various molecules across biological membranes (15, 16). There are 48 known human ABC transporters that are grouped into seven classes (16), and the ABCA and ABCG classes are believed to act as critical gatekeepers of cholesterol homeostasis (15–17). ABCG1 is the founding member of the ABCG subclass of ABC transporters (17, 18) and is widely expressed in several peripheral tissues as well as in gray and white matter in postnatal murine brain (19–21). Biochemically, ABCG1 facilitates cholesterol efflux to HDL but not to lipid-free apolipoprotein A-I (apoA-I) (21, 22) and redistributes intracellular cholesterol to plasma membrane domains that are accessible by cholesterol oxidase (23). Both the cholesterol efflux and distribution activities are present when ABCG1 is selectively expressed in cells, demonstrating that ABCG1 can function as a homodimer (21–23). Deficiency of ABCG1 in mice results in the accumulation of sterols within liver and macrophage-rich tissues when animals are challenged with a high-fat, high-cholesterol diet (24). ABCG1 is also highly expressed in brain and has been proposed to be a better correlate of cholesterol efflux from glia than ABCA1 (19–21, 25).

Intriguingly, the human *ABCG1* gene resides on chromosome 21 (26–29), suggesting that it may be of interest for some of the clinical phenotypes associated with Down syndrome (DS). DS is caused by inheritance of an extra copy of all or part of chromosome 21 and occurs in ~1 in 700 live births. Most individuals (95%) with DS are trisomic for the entire chromosome 21, which contains 337 genes whose individual roles in the syndrome are largely unknown (30). Analysis of DS individuals with partial trisomy 21 has shown that a “critical region” between loci D21S58 and D21S42 accounts for mental retardation and most of the facial features of DS (31–34).

One prominent phenotype in DS is the inevitable development of AD neuropathology, including parenchymal and cerebrovascular amyloid plaques and neurofibrillary tangles, by the mid to late 30s (35, 36). This is decades earlier than in the general population, who typically exhibit signs of AD in the mid to late 70s (36, 37). The onset of clinical dementia in DS is age-dependent, with prevalence rates of ~9% between 40 and 49 years, 36% between 50 and 59 years, and 55% between 60 and 69 years (38).

The human *APP* gene maps to chromosome 21q21.3, and two seminal observations demonstrate the pivotal role of *APP* gene dose in determining the age of onset of AD. First, excess *APP* is required for the accelerated onset of AD in DS (39). This was shown by the identification of a 78 year old DS subject who exhibited no amyloid deposition upon autopsy and who had partial trisomy 21 in which the chromosomal breakpoint excluded *APP* (39). More recently, five independent kindreds were identified that contain a duplication of the *APP* locus in the absence of mental retardation and other aspects of DS (40). These families all exhibit autosomal dominant early-onset AD with an average clinical age of onset of 52 years, and they exhibit abundant amyloid deposition in the parenchyma and cerebrovasculature (40). Together, these studies

conclusively demonstrate that *APP* gene dose critically regulates the age of onset of AD.

However, these studies do not rule out the possibility that other genes on chromosome 21 may also contribute to the decreased age of onset of AD neuropathology in DS subjects. Notably, there is evidence for a poorly understood locus on chromosome 21 that affects the risk and age of onset for sporadic AD (41), and it is possible that inheritance of extra copies of genes near this region may functionally synergize with excess *APP* and provide a better explanation for the greatly accelerated onset of AD neuropathology in DS than *APP* gene dose alone.

Therefore, we hypothesized that genes on chromosome 21 with known roles in lipid metabolism may be good candidates to participate in the development of early-onset AD neuropathology in DS. The human *ABCG1* gene maps to chromosome 21q.22.3 within the DS critical region and near the linkage peak that may affect onset and risk in sporadic AD (33, 41). Here, we show that the functional activity of ABCG1 as a cholesterol transporter influences the subcellular distribution and proteolytic processing of *APP*. Furthermore, we provide evidence of increased ABCG1 expression and increased proteolytic products of *APP* in DS cortex compared with normal controls. Our findings suggest the possibility that ABCG1 may contribute to the accelerated onset of AD neuropathology in DS.

## MATERIALS AND METHODS

### Cell culture and transfection

HEK293 cells stably expressing human *APP*<sub>695</sub> containing the Swedish mutation (HEK-*APP*<sub>swe</sub> cells) were cultured in growth medium (DMEM containing 10% FBS, 2 mM L-glutamine, 100 U/ml penicillin-streptomycin, and 200 µg/ml geneticin; all reagents from Canadian Life Technologies). Cells were transfected with a human ABCG1 cDNA (Image Consortium), a murine ABCG1 cDNA, or empty vector using Fugene (Roche) according to the manufacturer's recommendations.

### Measurement of A $\beta$ and sAPP species

Secreted human A $\beta$ <sub>1-40</sub> and A $\beta$ <sub>1-42</sub> was measured by ELISA (Biosource). For experiments involving transfected HEK-*APP*<sub>swe</sub> cells, medium was changed at 24 h after transfection and conditioned for 6–32 h. Conditioned medium was collected, mixed with Complete Protease Inhibitor (Roche), and frozen at –80°C until required. Samples were thawed only once. ELISA results, expressed as pg/ml, were normalized to total cellular protein to correct for variations in cell number. Time course experiments were conducted such that <10% of the total medium was removed over the course of the experiment in complete growth medium. The rate of A $\beta$  secretion was determined using Vernier Logger Pro (version 3.3) to generate quadratic curves to fit the data according to the criteria for the least possible slope error. The derivatives of these functions were evaluated over the interval 0–10 h. A $\beta$  levels measured during cholesterol efflux assays were obtained from cells conditioned for 6 h in DMEM and 0.2% delipidated BSA to maintain the identical conditions used in the cholesterol efflux assay (see below). For measurement of sAPP species, culture supernatants were normalized for total cellular protein to correct for variations in cell number

and immunoblotted with 6E10 (Chemicon) to detect sAPP $\alpha$  and with 10321 (Phoenix Biotech) to detect sAPP $\beta$ .

### Purification of HDL

HDL was purified by KBr density gradient ultracentrifugation from plasma obtained from normolipidemic human donors. Fractions corresponding to HDL<sub>2</sub> (1.063–1.125 g/ml) and HDL<sub>3</sub> (1.125–1.225 g/ml) were collected, pooled, and dialyzed against 15 mM NaCl and 0.1 mM EDTA overnight, followed by filter sterilization. Protein levels were determined by Lowry assay.

### Cholesterol efflux assay

Cells were seeded at 250,000 cells/well on 24-well plates and labeled with 1  $\mu$ Ci/ml [<sup>3</sup>H]cholesterol (New England Nuclear) for 18–24 h during transfection in growth medium. Labeled and transfected cells were washed once with serum-free DMEM, and 25  $\mu$ g/ml HDL<sub>2/3</sub> was added as a lipid acceptor in serum-free DMEM containing 0.2% delipidated BSA. Medium was collected 6 h later and centrifuged at 8,000 rpm to remove cell debris. Cells were lysed with 50  $\mu$ l of 0.1 M NaOH and 0.2% SDS and incubated at room temperature for 20 min. Fifty microliters of medium and cell lysate was added to scintillation plates and counted. Percentage cholesterol efflux was calculated as total counts in the medium divided by the sum of the counts in the medium plus the cell lysate (42).

### Western blotting

HEK-APP<sub>sw</sub>e cells were lysed in 10% glycerol, 1% Triton X-100, and Complete Protease Inhibitor (Roche) in PBS and centrifuged for 5 min at 9,000 rpm. Equal amounts of protein, determined by Lowry assay, were resolved through 7.5% or 10% SDS polyacrylamide gels, transferred to polyvinylidene fluoride membranes (Millipore), and immunodetected with 6E10. Nitrocellulose membranes (Millipore) were used in conjunction with anti-ABCG1 (Novus). Anti-GAPDH (Chemicon) was used as an internal protein-loading control. Blots were developed using enhanced chemiluminescence (Amersham) according to the manufacturer's recommendations.

For analyses of APP C-terminal fragments (CTFs), cells were lysed in RIPA buffer consisting of 20 mM Tris-HCl, pH 7.4, 5 mM EDTA, 50 mM NaCl, 10 mM Na-pyrophosphate, 50 mM NaF, 1% Nonidet-P40, and Complete Protease Inhibitor. Lysates were sonicated for 20 s and centrifuged for 5 min at 11,000 g, and the supernatants were collected. Thirty micrograms of protein was loaded per lane on 4% to 10% to 17% step gradient Tris-Tricine gels with an anode buffer consisting of 0.2 M Tris-HCl, pH 8.9, and a cathode buffer consisting of 0.1 M Tris-HCl, pH 8.4, 0.1 M Tricine, and 0.1% SDS. After electrophoresis, proteins were transferred to nitrocellulose membranes and probed with anti-APP C-terminal (Sigma) antibodies to detect CTF $\alpha$  or CTF $\beta$ .

For analysis of APP and ABCG1 protein expression in tissues, total membranes were purified as described (43). Tissues were homogenized in 5 volumes of lysis buffer (50 mM mannitol, 2 mM EDTA, 50 mM Tris-HCl, pH 7.6, and Complete Protease Inhibitor) and centrifuged at 500 g to pellet nuclei and debris. Between 400 and 450  $\mu$ l of supernatant was layered onto 600  $\mu$ l of fractionation buffer (300 mM mannitol, 2 mM EDTA, and 50 mM Tris-HCl, pH 7.6) and centrifuged at 100,000 g for 45 min to pellet total membranes. Membranes were resuspended in 150–200  $\mu$ l of lysis buffer. SDS was added to a final concentration of 1% before SDS-PAGE and immunoblotting with antibodies against APP, ABCG1, and NaK-ATPase as an internal loading control (Novus).

### Biotinylation assay

HEK-APP<sub>sw</sub>e cells were transfected with vector, murine ABCG1, or human ABCG1 for 24 h. Cells were washed twice with cold PBS and treated with 1 mg/ml sulfo-NHS-Biotin (Pierce) in PBS for 30 min at 4°C, washed twice with cold PBS, and quenched with cold 3.75 mg glycine/ml PBS. Cells were solubilized with lysis buffer (50 mM Tris-HCl, pH 7.5, 150 mM NaCl, 0.5% Triton X-100, and Complete Protease Inhibitor) for 30 min on ice, sonicated, and centrifuged at 14,000 rpm for 5 min at 4°C. Ten percent of the lysate was saved for analysis of total APP. Streptavidin-agarose beads (Pierce) were washed twice in lysis buffer, added to the remaining lysate, and rocked at 4°C overnight. Beads were collected by centrifugation and washed three times in 10 volumes of lysis buffer. Total and cell surface fractions were separated by SDS-PAGE and immunodetected for APP and actin as a loading control.

### Density gradient fractionation

HEK-APP<sub>sw</sub>e cells were transfected with vector or ABCG1 for 24 h. Cells were harvested, lysed, and fractionated over a continuous 0.58–1.1 mol/l sucrose density gradient as described (44, 45).

### Human tissues

Frozen human postmortem control, DS, and AD frontal cortex tissue samples were obtained from the University of Maryland Brain and Tissue Bank for Developmental Disorders (Baltimore, MD; National Institutes of Health contract N01 HD-1-3138) and the University of British Columbia Kinsman Laboratory Brain Bank (generously provided by Dr. Pat McGeer) in accordance with University of British Columbia and BC Children's Hospital clinical ethical approval. Each DS and AD sample was individually matched to a control for age, sex, and, wherever possible, ethnic background and postmortem interval (Table 1).

### RNA isolation and analysis

RNA from human brain tissues was extracted using Trizol (Invitrogen) according to the manufacturer's protocol. RNA samples were treated with DNaseI before cDNA synthesis. cDNA was generated using oligo-dT primers and TaqMan reverse transcription reagents (Applied Biosystems). Primers were designed using PrimerExpress software (Applied Biosystems) and spanned exons 22 and 23 of human ABCG1. Sequences are as follows: human ABCG1 forward (5'-ACACCATCCCCACGTACCTA-3') and reverse (5'-GATGACCCCTTCGAACCCA-3'); human APP forward (5'-GCTGGCTGAACCCAGATT-3') and reverse (5'-CCCACTTCCATTCTGGACAT-3') and human GAPDH forward (5'-CCTGCACCACCAACTGCTTA-3') and reverse (5'-CATGAGT-CCTTCCACGATACCA-3'). Quantitative RT-PCR was done with SYBR Green reagents (Applied Biosystems) on an ABI 7000. Cycling conditions were 50°C for 2 min, 95°C for 10 min, then 40 cycles at 95°C for 15 s and 60°C for 1 min, followed by dissociation at 95°C for 15 s, 60°C for 20 s, and 95°C for 15 s. Each sample was assayed in triplicate, normalized to GAPDH, and analyzed with 7000 system SDS software version 1.2 (Applied Biosystems) using the relative standard curve method.

### ELISA procedures to measure sAPP $\beta$ , sAPP $\alpha$ , full-length APP, and A $\beta$ in brain homogenates

Human brain homogenates prepared in 5.5 M guanidine-HCl were diluted 25-fold into PBS containing 2% BSA and 0.05% Tween-20. Purified human recombinant sAPP $\beta$ , sAPP $\alpha$ , and full-length APP<sub>695</sub> were used for standard curves in each ELISA for



TABLE 1. Human tissues

Type	Sample Identifier	Age	Sex	Ethnicity	PMI	Type	Sample Identifier	Age	Sex	Ethnicity	PMI
Control	1793	11	Male	AA	19	DS	1267	10	Male	AA	15
Control	1037	19	Male	C	11	DS	1960	19	Male	AA	14
Control	777	22	Male	AA	4	DS	707	22	Male	AA	15
Control	1441	31	Male	C	28	DS	753	23	Male	C	24
Control	1134	41	Male	C	15	DS	1258	44	Female	C	13
Control	1454	47	Female	C	24	DS	4659	46	Female	C	7
Control	4640	47	Female	C	5	DS	3233	47	Female	ND	20
Control	1113	56	Male	C	17	DS	3572	51	Male	C	20
Control	1206	57	Male	C	16	DS	1623	56	Male	C	7
Control	1444	79	Female	C	14	AD	1252	78	Male	C	9
Control	4534	70	Male	AA	28	AD	1172	79	Female	C	12
Control	4546	86	Female	C	22	AD	1312	87	Female	C	7
Control	1113	56	Male	C	17	AD	1562	83	Female	C	6
Control	1206	57	Male	C	16	AD	1630	84	Female	C	5
Control	1441	51	Male	C	28	AD	200	68	Male	ND	5
Control	1454	47	Female	C	24	AD	429	85	Female	ND	16
Control	1134	41	Male	C	15	AD	413	73	Female	ND	24

AA, African American; AD, Alzheimer's disease; C, Caucasian; DS, Down syndrome; ND, not determined; PMI, post mortem interval.

quantitation. Fifty microliters of each sample was loaded onto a half-area ELISA plate, precoated with 8E5, and incubated at 4°C overnight. The sAPP $\beta$  fragments were captured with the rabbit polyclonal 192wt (against peptide epitope ISEVKM). The sAPP $\alpha$  fragments were captured with the rabbit polyclonal 3436 (against peptide epitope YEVHHQK). Full-length APP was captured with the rabbit polyclonal Zymed anti-APP $\beta$  antibody. Goat anti-rabbit IgG conjugated with HRP was used as a reporting antibody. Human A $\beta$  was quantified in guanidine-solubilized extracts from brains as described previously (46).

#### ABCG1-deficient mice

ABCG1-deficient mice were obtained from Deltagen. The targeting vector used to generate these mice contained 7 kb of 5' and 1.4 kb of 3' murine genomic DNA flanking a 7 kb IRES-LacZ-Neo-pA cassette that places the  $\beta$ -galactosidase gene under the control of endogenous ABCG1 regulatory elements. Homologous recombination results in the deletion of seven amino acids (GPSGAGK) within the Walker A motif in exon 3 of the murine *abcg1* gene. Chimeric animals were generated using embryonic stem cells derived from the 129/OlaHsd genetic background and were backcrossed to C56Bl/6 mice for at least seven generations before use. All procedures involving experimental animals were performed in accordance with protocols from the Canadian Council of Animal Care and the University of British Columbia Committee on Animal Care.

#### Histology

Wild-type and ABCG1-hemizygous mice were perfused with PBS. Brains were postfixed in 2% paraformaldehyde in PBS for 24 h, rinsed with PBS, and cryoprotected in 20% sucrose in PBS overnight at 4°C. Frozen coronal sections (40  $\mu$ m) were prepared on a cryostat and mounted on Superfrost Plus (Fisher) slides. Slides were immersed in 1  $\mu$ g/ml 5-bromo-4-chloro-3-indolyl  $\beta$ -D-galactosidase for 2 h at 37°C and counterstained with Neutral Red. Bright-field images were captured on a Zeiss Axioplan microscope.

#### Statistical analysis

Data were analyzed by Student's *t*-test or one-way ANOVA with a Newman-Keuls posttest using GraphPad Prism software (version 4.0). All in vivo data were conducted with the rater blinded to genotype.

## RESULTS

### ABCG1 increases A $\beta$ levels

To determine whether ABCG1 affects the secretion of A $\beta$  peptides, HEK293 cells stably expressing APP<sub>695</sub> containing the Swedish mutation (HEK-APP<sub>swe</sub> cells) were transiently transfected with empty vector or human ABCG1 cDNA, and the levels of A $\beta$ 40 and A $\beta$ 42 released into the medium were measured over time. We observed a consistent increase in secreted A $\beta$ 40 and A $\beta$ 42 levels throughout the course of these experiments. For example, the level of A $\beta$ 40 secreted from HEK-APP<sub>swe</sub> cells expressing ABCG1 was 1.8-fold greater than that of the vector-only control at 10 h ( $P < 0.0001$ ,  $n = 2$ ) (Fig. 1A), and the level of A $\beta$ 42 was 2.1-fold greater than that of the vector control at 10 h ( $P < 0.0001$ ,  $n = 2$ ) (Fig. 1B). Western blot analysis demonstrated that ABCG1 was undetectable in vector-transfected HEK-APP<sub>swe</sub> cells but was abundant in cells expressing ABCG1 (Fig. 1C). These data show that the levels of A $\beta$  released from HEK-APP<sub>swe</sub> cells is augmented in the presence of ABCG1.

### Functional ABCG1 is required for increased A $\beta$ secretion

To determine whether the enzymatic function of ABCG1 as a cholesterol transporter (21–23) is required for increased A $\beta$  secretion, HEK-APP<sub>swe</sub> cells were transfected with empty vector, wild-type ABCG1, or ABCG1 containing an S220G mutation in the ATP binding cassette signature motif that is conserved in mouse, rat, dog, and *Drosophila melanogaster*. As expected, the S220G mutation reduced the cholesterol efflux activity of ABCG1 to that of the vector-only controls (Fig. 2A). Notably, this mutation also reduced A $\beta$ 40 and A $\beta$ 42 secretion to baseline levels (Fig. 2B, C), demonstrating that the ability of ABCG1 to augment A $\beta$  release requires its function as a cholesterol transporter.

### ABCG1 also increases sAPP $\alpha$ and sAPP $\beta$ secretion

To determine the effect of ABCG1 on the release of sAPP species, we next evaluated the levels of sAPP $\alpha$  and sAPP $\beta$  in conditioned medium from HEK-APP<sub>swe</sub> cells

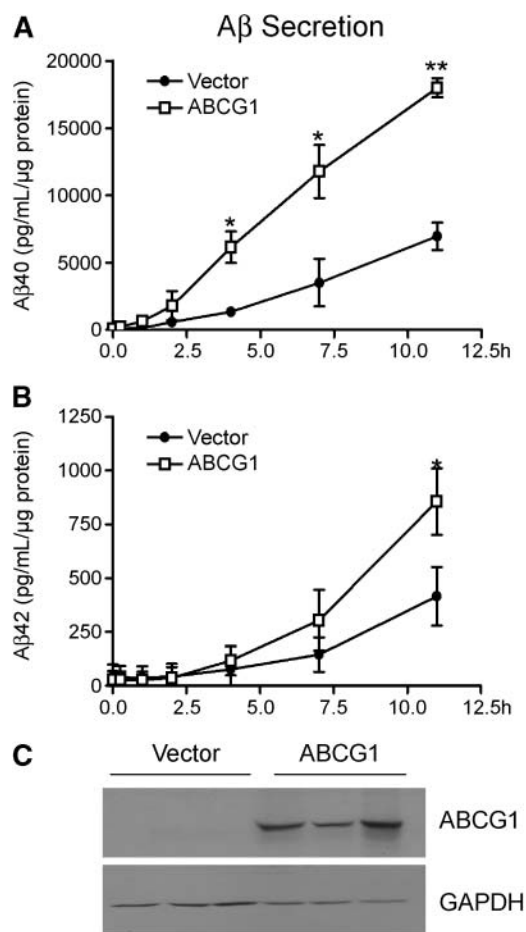


**Fig. 1.** ABCG1 enhances amyloid- $\beta$  protein ( $A\beta$ ) production in vitro. A, B: HEK-APPsw cells were transiently transfected with empty vector or ABCG1. Conditioned medium was collected at various times, assayed for  $A\beta$ 40 (A) and  $A\beta$ 42 (B) by ELISA, and normalized to total cell protein. Data represent means  $\pm$  SD of two independent experiments for empty vector and ABCG1. Data were analyzed by unpaired Student's *t*-test at each time point; \*  $P < 0.05$ , \*\*  $P < 0.01$ . C: Western blot shows the detection of ABCG1 protein after transfection with ABCG1.

expressing empty vector or ABCG1. Intriguingly, a significant increase in sAPP $\alpha$  (63% above control;  $P = 0.020$ ,  $n = 3$ ) as well as increased sAPP $\beta$  (73% above control;  $P = 0.002$ ,  $n = 3$ ) was observed in the presence of ABCG1 relative to vector (**Fig. 3**). These observations suggest that ABCG1 may lead to an increase in the availability of APP as a substrate for both  $\alpha$ -secretase and  $\beta$ -secretase pathways. APP mRNA levels were unchanged in HEK-APPsw cells expressing vector (APP/GAPDH ratio =  $1.076 \pm 0.265$ ;  $n = 3$ ) and ABCG1 (APP/GAPDH ratio =  $1.002 \pm 0.074$ ;  $n = 3$ ), demonstrating that increased transcription of APP per se cannot account for the increased production of secretase products.

#### CTF $\alpha$ and CTF $\beta$ levels are increased in cells expressing ABCG1

CTF $\alpha$  and CTF $\beta$  fragments were next analyzed by Western blot in transfected HEK-APPsw cells. Compared with vector, ABCG1-expressing cells exhibited a significant increase in CTF $\alpha$  ( $P = 0.0137$ ,  $n = 3$ ) and CTF $\beta$  ( $P = 0.0066$ ,  $n = 3$ ),

which remained even when corrected for the increase in total APP observed in ABCG1-expressing cells (CTF $\alpha$ /APP,  $P = 0.0136$ ,  $n = 3$ ; CTF $\beta$ /APP,  $P = 0.0002$ ,  $n = 3$ ) (**Fig. 4**). Although a proportional increase in CTF $\alpha$  and CTF $\beta$  can be caused by decreased  $\gamma$ -secretase activity, our observation that CTF $\alpha$  and CTF $\beta$  levels are both increased suggests that expression of ABCG1 promotes increased processing of APP by both the amyloidogenic and non-amyloidogenic pathways.

#### ABCG1 increases cell surface presentation of APP

Although the precise intracellular sites of APP proteolysis is a subject of considerable debate, it has been reported that all secretases have the ability to cleave APP at the cell surface and/or in early endosomes (47–50). Because ABCG1 is known to influence the distribution of cholesterol at the plasma membrane (23) and affects both the  $\alpha$ -secretase and  $\beta$ -secretase pathways of APP processing, we hypothesized that ABCG1 could increase the proportion of APP at the cell surface that is available for proteolysis by all secretases either at the cell surface or upon endocytosis. Therefore, biotinylation assays were used to determine the subcellular distribution of APP in ABCG1-expressing cells. HEK-APPsw cells expressing either murine or human ABCG1 exhibited increased total APP ( $P = 0.009$  for murine vs. control,  $P = 0.003$  for human vs. control,  $n = 3$ ) and increased surface APP ( $P = 0.01$  for murine vs. control,  $P = 0.0003$  for human vs. control,  $n = 3$ ). Notably, the increase in surface APP was greater than the increase in total APP, resulting in an increased proportion of total APP at the plasma membrane ( $P = 0.097$  for murine vs. control,  $P = 0.008$  for human vs. control,  $n = 3$ ). These results show that the increased cell surface APP was only partly accounted for by the increase in total APP levels in ABCG1-expressing cells (**Fig. 5**), suggesting that ABCG1 activity preferentially presents APP at the cell surface. Furthermore, continuous sucrose density centrifugation and Western blot analysis showed that an increased proportion of APP colocalized with a plasma membrane marker ( $\beta$ 1-integrin) in ABCG1-expressing compared with control HEK-APPsw cells (data not shown). These results from two independent methods indicate that modulation of the intracellular lipid environment by ABCG1 increases the cell surface presentation of APP.

To test whether increased cell surface APP could be attributed to the adherence of secreted APP species to the plasma membrane, HEK293 cells that did not express APPsw were transfected with vector or ABCG1 for 24 h to allow for ABCG1-mediated changes in cell surface lipid distribution to occur, then exposed for an additional 24 h to conditioned medium containing sAPP. Neither vector-transfected nor ABCG1-expressing cells accumulated detectable sAPP (**Fig. 6**), suggesting that ABCG1-mediated changes in membrane composition are not sufficient to attract exogenous sAPP to the cell surface.

#### ABCG1 is highly expressed in neurons and is overexpressed in DS frontal cortex

Homologous recombination of an IRES-LacZ-Neo-pA cassette into the murine *abcg1* locus allows rapid analysis of

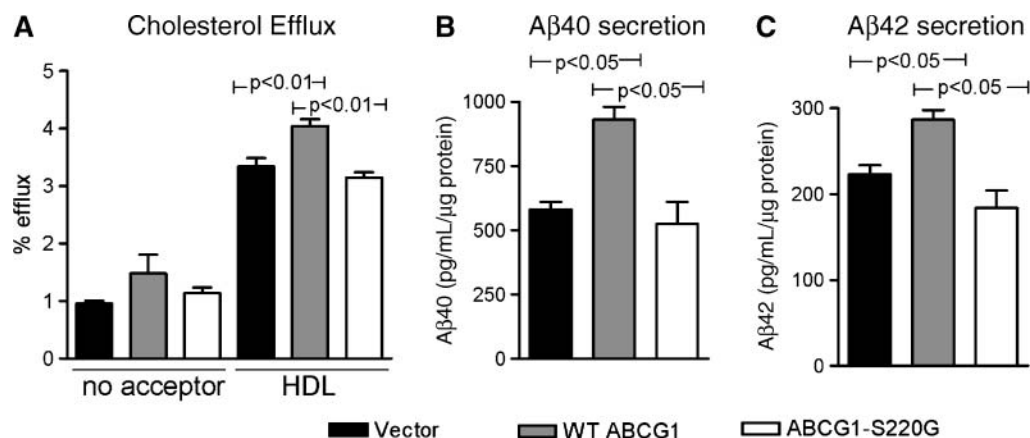


**Fig. 2.** ABCG1 requires cholesterol efflux activity to affect A $\beta$  production. HEK-APP<sup>sw</sup> cells were transfected with vector, wild-type (WT) ABCG1, or ABCG1 containing a S220G mutation in the Walker A domain. A: Wild-type ABCG1, but not ABCG1 S220G, effluxes cholesterol to exogenous HDL above baseline levels. Data represent means  $\pm$  SEM from at least two independent cholesterol efflux assays over a 6 h period, each measured in triplicate. B, C: Wild-type ABCG1, but not ABCG1 S220G, augments A $\beta$ 40 (B) and A $\beta$ 42 (C) production above baseline levels. Data represent means  $\pm$  SEM of at least two independent experiments.

ABCG1 expression patterns using  $\beta$ -galactosidase histological staining. Analysis of hemizygous ABCG<sup>+/-</sup> brains demonstrated that ABCG1 is highly expressed in neurons, with particularly abundant expression in hippocampus, where it is found in CA1, CA2, and CA3 neurons as well as in the dentate gyrus. ABCG1 is also expressed in all cortical layers as well as in the striatum and thalamus (Fig. 7).

Quantitative RT-PCR was then used to measure the levels of human ABCG1 mRNA from eight postmortem trisomy 21 patients who ranged in age from 10 to 56 years

(Table 1). Each trisomy 21 patient was matched by age and sex to a normal control (Table 1). ABCG1 mRNA abundance was also quantified from eight late-onset AD patients who were also matched by age and sex to a normal control (Table 1). ABCG1 mRNA levels in DS frontal cortex were 2.435  $\pm$  1.43-fold more abundant than in control frontal cortex ( $P = 0.023$ ,  $n = 8$ ) (Fig. 8), clearly demonstrating that inheritance of an extra copy of ABCG1 is associated with increased ABCG1 mRNA levels in human postmortem trisomy 21. Notably, no significant difference was observed between ABCG1 mRNA levels in AD brain compared with age- and sex-matched controls ( $P = 0.911$ ,  $n = 11$ ), showing that the presence of AD neuropathology is not sufficient to upregulate ABCG1 expression. In contrast to ABCG1, we found that APP mRNA levels were not increased significantly in these same trisomy 21 patients relative to controls, although a clear trend toward increased APP expression was observed ( $P = 0.131$ ,  $n = 8$ ). APP mRNA levels were indistinguishable in AD patients compared with controls ( $P = 0.846$ ,  $n \geq 7$ ) (Fig. 8B).

Western blot analysis of total membrane preparations revealed that ABCG1 protein levels were 2-fold more abundant in DS frontal cortex compared with those in age-matched controls ( $P = 0.008$ ,  $n = 4$ ) (Fig. 9). In contrast, APP protein levels were not significantly different in these same fractions ( $P = 0.638$ ,  $n = 4$ ) (Fig. 9).

### A $\beta$ and sAPP $\alpha$ levels are increased in DS cortex

Finally, we determined whether excess ABCG1 in DS is associated with increased processing of APP in vivo. First, total A $\beta$ 40 and A $\beta$ 42 levels were assessed in 9 trisomy 21 patients relative to 10 controls. As expected, both A $\beta$ 40 and A $\beta$ 42 were increased significantly in DS cortex ( $P = 0.031$  and  $P = 0.005$ , respectively) (Fig. 10A). Next, total APP and sAPP levels were quantified in these same DS and control patients. In whole cortical lysates, total APP protein levels as measured by ELISA were indistinguishable

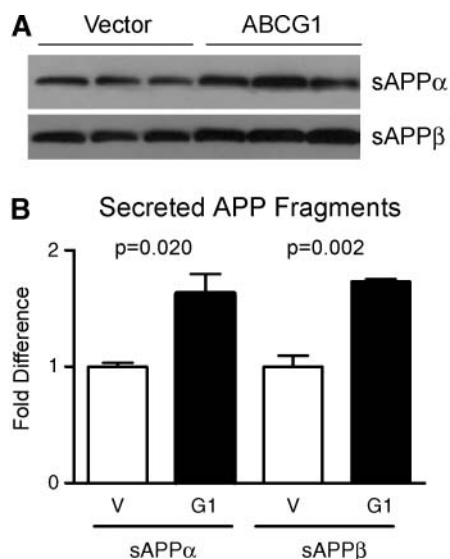


**Fig. 3.** ABCG1 promotes the release of secreted of  $\beta$ -amyloid precursor protein (sAPP $\alpha$  and sAPP $\beta$ ). A: HEK-APP<sup>sw</sup> cells were transfected with ABCG1 or empty vector for 24 h, followed by a 6 h period of conditioning in fresh medium. sAPP $\alpha$  and sAPP $\beta$  levels were evaluated by Western blot analysis of medium and normalized to total cellular protein. B: The graph represents means  $\pm$  SEM of a representative experiment from three independent transfections. G1, ABCG1; V, vector.



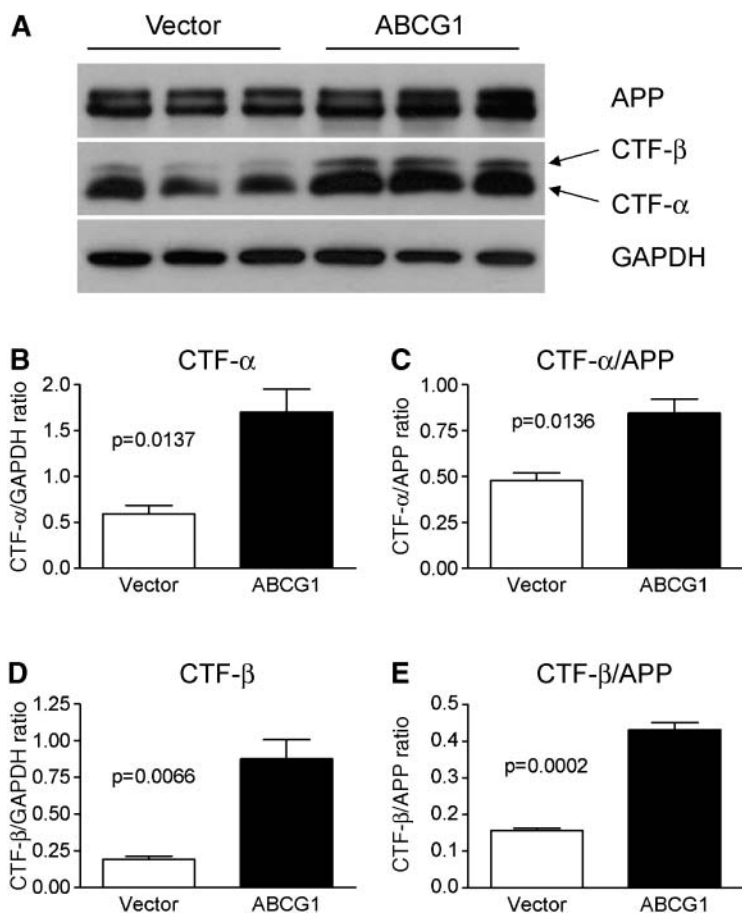


**Fig. 4.** ABCG1 enhances  $\alpha$ -secretase and  $\beta$ -secretase cleavage of APP. A: Representative Western blot of total APP as well as C-terminal fragment  $\alpha$  (CTF $\alpha$ ) and CTF $\beta$  from HEK-APP<sub>sw</sub> cells transfected with vector. B–E: The graphs represent means  $\pm$  SEM of three transfections. B, D: Total CTF levels corrected for GAPDH. C, E: CTF levels corrected for total APPs. A total of three independent rounds of transfections, each at least in triplicate, were performed.

in trisomy 21 patients compared with controls (Fig. 10B). The levels of sAPP $\beta$  did not differ significantly between DS and control patients, irrespective of whether the sAPP $\beta$  measurement was normalized for total APP protein level in each patient (Fig. 10C, D). In contrast, sAPP $\alpha$  levels tended to be increased in DS cortex compared with controls ( $P = 0.063$ ), which was significant when corrected for total APP levels for each patient ( $P = 0.024$ ) (Fig. 10E, F). These results show that expression of excess ABCG1 is associated with increased A $\beta$  and sAPP $\alpha$  levels in DS brain.

## DISCUSSION

Intracellular cholesterol levels markedly affect APP processing and the subcellular distribution of APP and secretase components (4–14). However, little is known about how genes that control intracellular lipid distribution may affect APP metabolism. Here, we demonstrate that transient expression of the cholesterol transporter ABCG1 affects the proteolytic processing and subcellular distribution of APP in vitro. In cultured HEK-APP<sub>sw</sub> cells, expression of functional ABCG1 increases A $\beta$ , sAPP $\alpha$ , and sAPP $\beta$  secretion and increases the proportion of APP that is present at the cell surface. Because APP and secretases are all membrane-bound proteins whose subcellular distribution and activities are highly dependent on cholesterol (6, 51–53), it is

possible that the activities of ABCG1 in lipid trafficking and efflux may influence the intracellular routing of several gene products involved in APP metabolism. Our observations provide evidence for a novel activity of ABCG1 as a modulator of APP processing and subcellular trafficking and suggest that ABCG1 may be a key participant in pathways that link cholesterol with APP metabolism.

Observations that increased cholesterol augments A $\beta$  production (4–7), whereas cholesterol depletion stimulates  $\alpha$ -secretase activity (8–13), have led to the prediction that genes such as ABCG1 and ABCA1 that promote cholesterol efflux should decrease A $\beta$  levels by the resulting reduction of intracellular sterol content. However, investigations of both ABCG1 and ABCA1 suggest that this prediction may be overly simplistic and that effects on intracellular cholesterol distribution may be equally important in modulating APP processing as cholesterol levels.

ABCA1 is crucial for the efflux of cholesterol onto lipid-poor apolipoprotein particles (54). Deficiency of ABCA1 leads to the accumulation of intracellular cholesterol and a nearly complete lack of circulating HDL (55–57). Although early in vitro studies suggested that ABCA1 influences A $\beta$  production, no consensus was reached on whether ABCA1 increased or decreased A $\beta$  levels (58–60). Furthermore, four independent groups have now demonstrated in vivo that A $\beta$  levels are unaffected by the absence of ABCA1 (61–64). We and others have recently shown

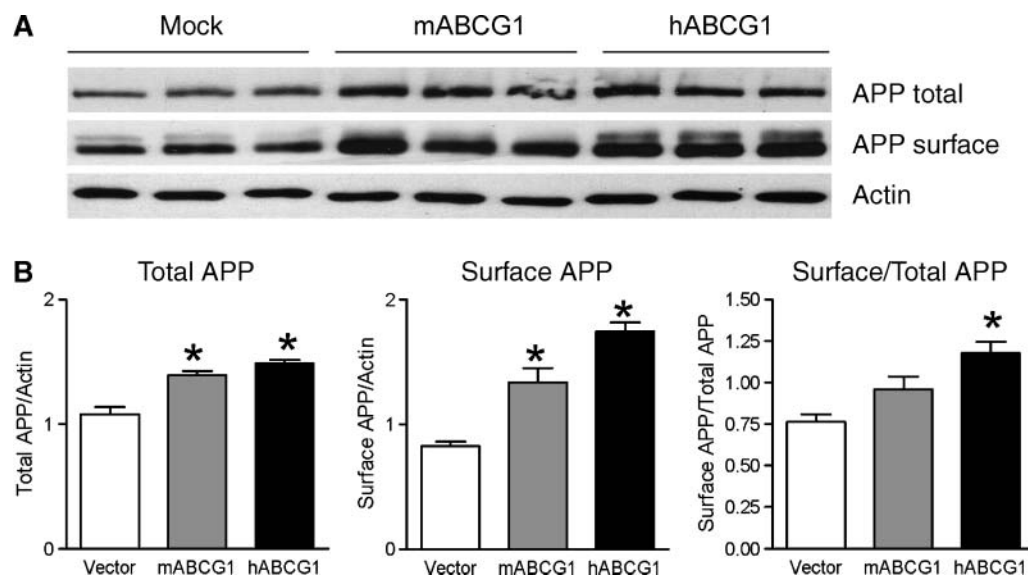


**Fig. 5.** ABCG1 increases cell surface presentation of APP. **A:** Representative Western blot of HEK-APP<sup>swe</sup> cells transiently transfected with empty vector, murine ABCG1, or human ABCG1 and treated with sulfo-NHS-biotin followed by precipitation of biotinylated cell surface proteins using streptavidin agarose beads. The levels of total and cell surface APP are shown and normalized to actin levels as an internal control. **B:** Quantitation of APP distribution. The graphs represent means  $\pm$  SEM of a representative round from three independent transfections, analyzed by Student's *t*-test. Three rounds of at least triplicate independent transfections were performed. Asterisks represent  $P < 0.05$ .

that ABCA1 influences amyloidogenesis via alterations in apoE metabolism. Mice lacking ABCA1 have severe reductions in apoE levels in the brain, which results from inefficient secretion and lipidation of apoE from glia (65, 66). Importantly, these poorly lipidated apoE particles greatly facilitate the formation of amyloid deposits (61–63). Together, these studies demonstrate that although one function of ABCA1 is to modulate cholesterol levels, ABCA1 does not appear to modulate A $\beta$  production in vivo. Rather, these results suggest that ABCA1 influences amyloid deposition and/or clearance by affecting apoE levels and lipidation.

ABCG1 also promotes cholesterol efflux, but in contrast to ABCA1, ABCG1 can only transfer cholesterol to lipidated particles such as HDL (21, 22). Here, we provide evidence that ABCG1 also affects APP metabolism and that this requires its cholesterol efflux activity. Under our in vitro conditions, ABCG1 facilitates APP processing through both the  $\alpha$ -secretase and  $\beta$ -secretase pathways, leading to increased secretion of A $\beta$ , sAPP $\alpha$ , and sAPP $\beta$  species, which is associated with increased cell surface presentation of APP. Therefore, our results identify a novel function of ABCG1 as a modulator of APP trafficking in a cholesterol-dependent manner and categorize ABCG1 as

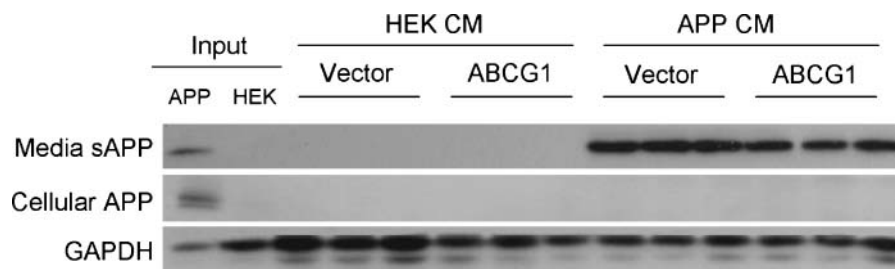


**Fig. 6.** ABCG1 does not increase the cellular adherence of exogenous sAPP. Conditioned medium and cell lysates were prepared from HEK-APP<sup>swe</sup> and HEK293 cells (input APP and HEK). HEK293 cells were transfected with vector or ABCG1 and exposed to conditioned medium from HEK293 cells (HEK CM) or conditioned medium from HEK-APP<sup>swe</sup> cells (APP CM) for 24 h, after which medium and cell lysates were immunoblotted for APP and GAPDH. The upper panel (Media sAPP) shows the input levels of sAPP in the conditioned medium at the beginning of the experiment and demonstrates no loss of input signal after 24 h of incubation on transfected cells. The middle panel (Cellular APP) shows the levels of cell-associated APP in HEK-APP<sup>swe</sup> and HEK293 cells (input lanes) and in HEK293 cells exposed to HEK293 CM or APP CM using 75  $\mu$ g of protein per lane. The lower panel shows GAPDH as an internal loading control.



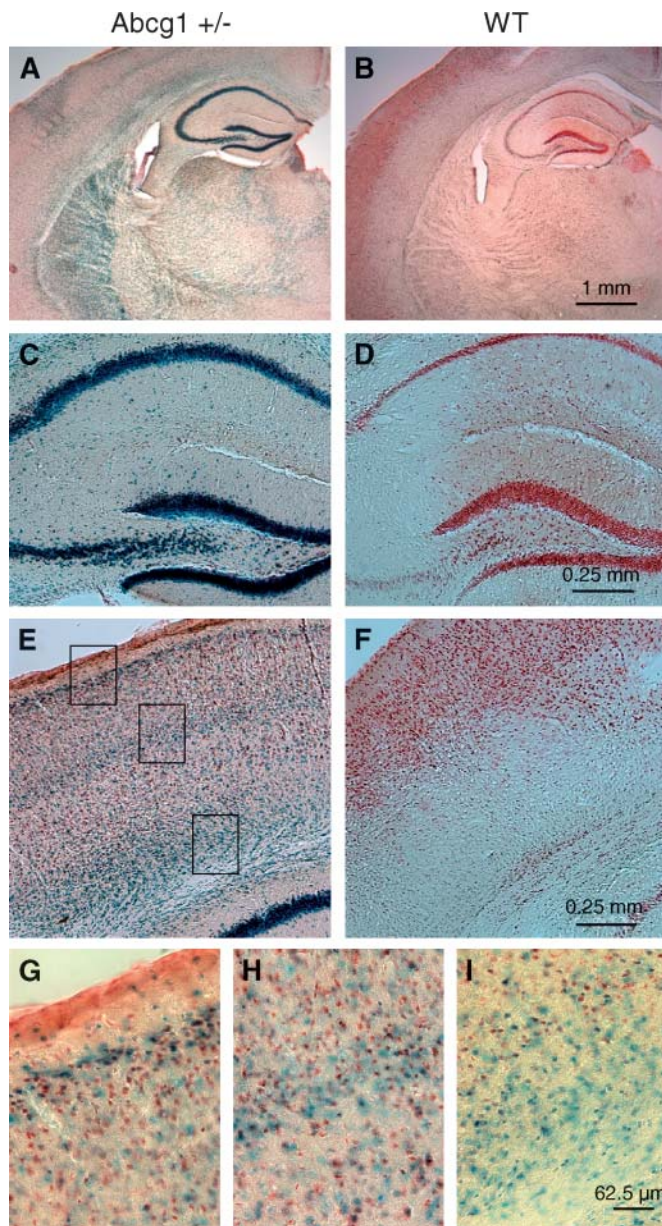


**Fig. 7.** ABCG1 is highly expressed in neurons. LacZ staining of ABCG1 heterozygous (A, C, E, G–I) and wild-type (WT; B, D, F) mice. Coronal sections are shown at 2.5 $\times$  (A, B), 10 $\times$  (C–F), and 40 $\times$  (G–I) magnification. Strong LacZ staining, indicative of ABCG1 expression, is observed in hippocampus (A, C), all cortical layers (A, E, G–I), striatum, and thalamus (A).

one of the first genes reported to increase APP presentation at the cell surface.

However, much remains to be learned. For example, it is not yet known whether ABCG1 may also affect the enzymatic activity of secretases that depend on a lipid environment, or whether it may simply influence the interaction of secretases and APP within specific membrane microdomains. We do not know whether ABCG1 may affect the trafficking of APP through anterograde, retrograde, or endocytic pathways. Finally, it is not known whether ABCG1 may contribute to the increased matura-

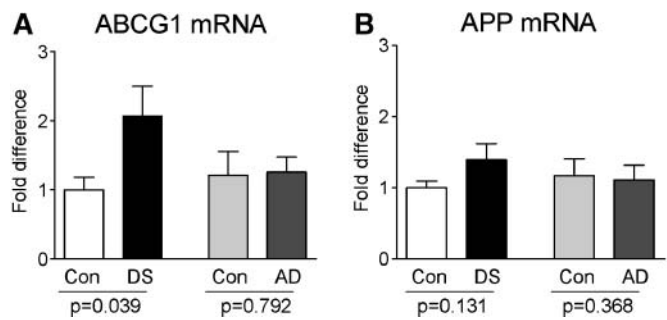


**Fig. 8.** ABCG1 mRNA levels are increased significantly in Down syndrome (DS) cortex. Quantitative RT-PCR was used to determine ABCG1 (A) and APP (B) mRNA levels from eight trisomy 21 patients (black bars) and eight age- and sex-matched controls (Con; white bars) as well as eight Alzheimer's disease (AD) patients (dark gray bars) and eight age- and sex-matched controls (light gray bars). Data represent means  $\pm$  SEM of each patient measured in duplicate for the DS patients and matched controls and in triplicate for the AD patients and matched controls, analyzed by Student's unpaired *t*-test.

tion of BACE1 that was recently identified as a novel mechanism contributing to AD in DS (67). Understanding the precise mechanisms by which ABCG1 leads to increased cell surface APP and subsequent processing will require evaluating each of these aspects of APP metabolism. Intriguingly, our results differ from a recent report suggesting that ABCG1 suppresses A $\beta$  production in CHO cells in a manner unrelated to its cholesterol efflux activity (68), although effects on CTF or sAPP generation

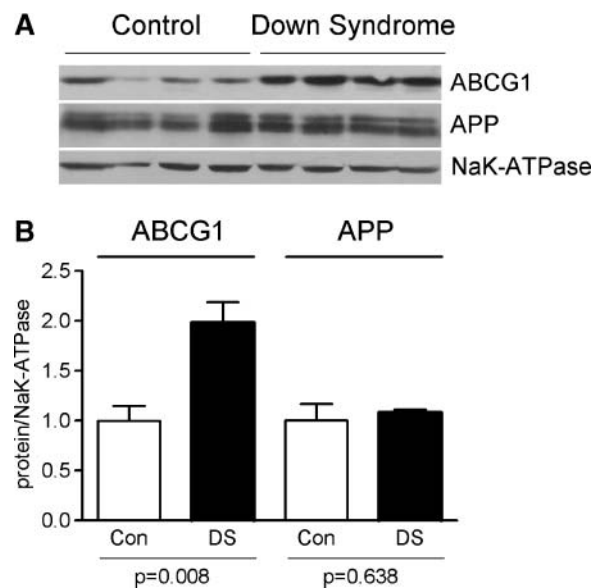


**Fig. 9.** ABCG1 protein levels are increased significantly in DS cortex. A: Western blots of total membrane fractions from four age-matched controls and trisomy 21 patients. Blots were probed sequentially for ABCG1, APP, and NaK-ATPase as an internal loading control. B: Relative ABCG1/NaK-ATPase and APP/NaK-ATPase values are shown, with the values in control (Con) fractions set to 1. Data represent means  $\pm$  SEM of each patient assayed in duplicate and analyzed by Student's unpaired *t*-test.

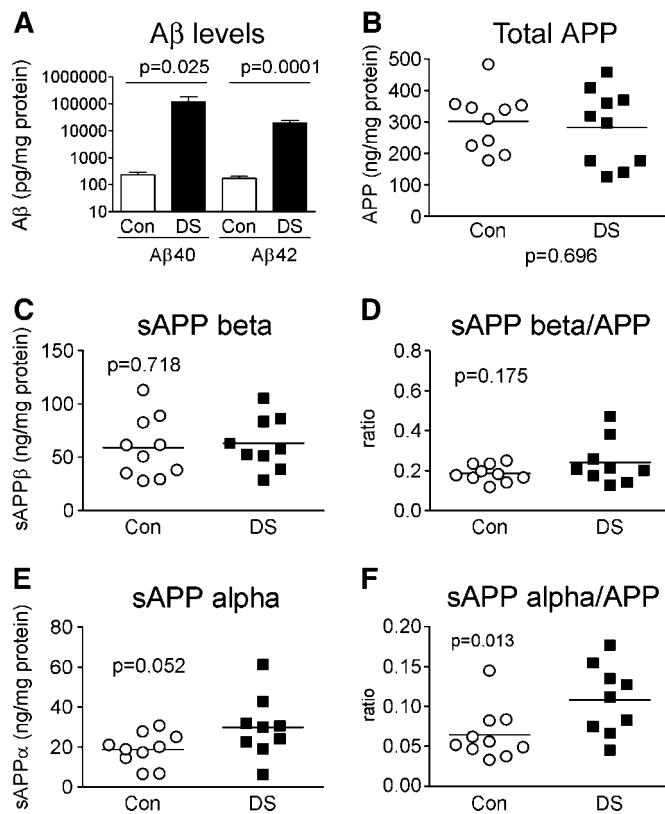


**Fig. 10.** A $\beta$  and sAPP $\alpha$  levels are increased in DS cortex. A: A $\beta$ 40 and A $\beta$ 42 levels were determined by ELISA in cortex of 9 trisomy 21 patients (DS) and 10 controls (Con). Data represent means  $\pm$  SEM. B: Total APP levels were quantified by ELISA from these same trisomy 21 patients and controls. C–F: sAPP $\beta$  (C, D) and sAPP $\alpha$  (E, F) were determined by ELISA from these same trisomy 21 patients and controls. Data are presented as scatterplots of sAPP $\beta$  and sAPP $\alpha$  levels expressed before (C, E) and after (D, F) normalization to APP levels in each brain sample, with horizontal lines representing the means.

and APP subcellular localization were not evaluated. As in the case with ABCA1, *in vivo* studies using mice with a selective increase or deficiency of ABCG1 will be required to evaluate the impact of ABCG1 on the pathogenesis of AD in an appropriate physiological context.

Our findings that DS cortex contains 2-fold more ABCG1 mRNA and protein than age-matched control samples and exhibits increased A $\beta$  and sAPP $\alpha$  levels are consistent with many of our observations in ABCG1-expressing HEK-APPsw cells. Unlike in HEK-APPsw cells, however, we did not observe increased sAPP $\beta$  levels in our cohort of DS postmortem tissue. Mechanisms for this could include increased  $\gamma$ -secretase activity or increased turnover of sAPP $\beta$  relative to sAPP $\alpha$  in DS tissue. Interestingly, a recent study reported that CTF $\alpha$  levels decline during aging in DS, whereas CTF $\beta$  levels increase (69). It is possible that we were unable to detect these changes given the relatively small number of DS samples of a wide age variation that were examined in this study. Finally, it is important to note that our *in vivo* results are correlative and do not rule out the possibility that other chromosome 21 genes in addition to ABCG1 may also play

a role in the development of early AD neuropathology in DS patients. Recently, BACE2, a novel aspartyl protease located on chromosome 21, was excluded as a potential gene that contributes to the development of AD neuropathology in DS (70). Future studies will be required to evaluate the impact of the selective overexpression or deficiency of ABCG1 on AD neuropathology *in vivo*.

It has long been established that excess APP is required to observe AD neuropathology in DS, as analysis of a single DS patient with partial trisomy 21 that excluded APP revealed no evidence of amyloid deposition at 78 years of age (39). Recently, duplication of the APP locus in five independent families was reported to cause autosomal dominant early-onset AD with cerebral amyloid angiopathy with a mean clinical age of onset of dementia by 52 years in 19 affected individuals (40). None of these affected individuals had other features of DS, such as mental retardation, before the onset of clinical dementia. However, the relationship between APP gene dose and APP expression in DS is not simple. Increased APP mRNA has been reported in fetal and adult DS brain (71–73), yet several studies have failed to observe significantly increased APP protein levels in DST compared with control brains (74–76). Immunohistochemical analysis of postnatal DS brain suggests that the neuronal staining intensity of APP protein increases during aging (75), although a recent study found no association between total APP levels and age (69). Interestingly, a survey of 41 genes on chromosome 21 demonstrated that APP exhibited the highest degree of interindividual variability of expression (77), suggesting that individual differences in APP expression levels may also partly account for the varying ability to detect APP overexpression in different DS patients. In our cohort, we failed to observe significant APP overexpression in DS cortex when evaluated by quantitative RT-PCR, Western blot, or ELISA. Although a clear trend toward increased APP mRNA levels was evident, total APP protein levels were similar in our DS and control cohorts.

In contrast to APP, we consistently observed a robust 2-fold increase in ABCG1 mRNA levels in DS compared with control cortex, consistent with published microarray findings that ABCG1 mRNA levels are increased by 1.43-fold in DS brain and by 1.23-fold in fetal DS cells (73, 78). ABCG1 protein levels were also 2-fold more abundant in DS brain compared with controls. These data clearly show that ABCG1 is overexpressed in DS, which may result in increased processing of APP beyond that accounted for solely by increased APP levels.

This study suggests that the accelerated onset of AD neuropathology in DS may also involve alterations in intracellular lipid trafficking mediated by overexpression of the cholesterol transporter ABCG1. ABCG1 is a half-sized transporter, and the results of several studies, including ours, have demonstrated that ABCG1 can function as a homodimer. This suggests that the inheritance of excess ABCG1 gene dose in DS may be sufficient to increase functional ABCG1 activity without necessarily invoking a requirement for increased levels of other half-sized transporters such as ABCG4 that may heterodimerize with



ABCG1. Here, we have demonstrated a novel property of ABCG1 in promoting the cell surface presentation of APP and leading to its increased proteolytic processing by secretases. In vivo, ABCG1 is highly expressed in neurons, overexpressed in DS brain, and associated with increased A $\beta$  and sAPP $\alpha$  levels in human postmortem tissue. Our observations support the hypothesis that excess ABCG1 in DS may result in an altered distribution of APP that facilitates the generation of neurotoxic A $\beta$  species and accelerates the onset of AD neuropathology. **■**

The authors are grateful to Pat McGeer for the generous contribution of banked AD and control postmortem tissues and to David Holtzman, Peter Reiner, and our research teams for invaluable input throughout the course of this work. B.L.B. and V.H.R. are supported by a graduate scholarship from the British Columbia Child and Family Research Institute and a postdoctoral fellowship from the Canadian Institutes of Health Research (CIHR), respectively. W.S. is supported by the Jack Brown and Family Alzheimer's Research Foundation, CIHR, and the Michael Smith Foundation for Health Research. N.W. is supported by National Institutes of Health Pilot Grant AG-08702-16. C.L.W. is supported by a CIHR New Investigator Salary Award and by operating grants from the Canadian Gene Cure Foundation, the BC Children's Hospital, CIHR (Grant MOP 67068), and the American Health Assistance Foundation.

## REFERENCES

- Price, D. L., R. E. Tanzi, D. R. Borchelt, and S. S. Sisodia. 1998. Alzheimer's disease: genetic studies and transgenic models. *Annu. Rev. Genet.* **32**: 461–493.
- Haass, C., and D. J. Selkoe. 1993. Cellular processing of  $\beta$ -amyloid precursor and the genesis of amyloid  $\beta$ -peptide. *Cell*. **75**: 154–159.
- Wolozin, B. 2004. Cholesterol and the biology of Alzheimer's disease. *Neuron*. **41**: 7–10.
- Refolo, L. M., M. A. Pappolla, B. Malester, J. LaFrancois, T. Bryant-Thomas, R. Wang, G. S. Tint, K. Sambamurti, and K. Duff. 2000. Hypercholesterolemia accelerates the Alzheimer's amyloid pathology in a transgenic mouse model. *Neurobiol. Dis.* **7**: 321–331.
- Shie, F. S., L. W. Jin, D. G. Cook, J. B. Leverenz, and R. C. LeBoeuf. 2002. Diet-induced hypercholesterolemia enhances brain A beta accumulation in transgenic mice. *Neuroreport*. **213**: 455–459.
- Wahrle, S., P. Das, A. C. Nyborg, C. McLendon, M. Shoji, T. Kawarabayashi, L. H. Younkin, S. G. Younkin, and T. E. Golde. 2002. Cholesterol-dependent  $\gamma$ -secretase activity in buoyant cholesterol-rich membrane microdomains. *Neurobiol. Dis.* **9**: 11–23.
- Burns, M., K. Gaynor, V. Olm, M. Mercken, J. LaFrancois, L. Wang, P. M. Matthews, W. Noble, Y. Matsuoka, and K. Duff. 2003. Presenilin redistribution associated with aberrant cholesterol transport enhances  $\beta$ -amyloid production in vivo. *J. Neurosci.* **23**: 5645–5649.
- Fassbender, K., M. Simons, C. Bergmann, M. Stroick, D. Lütjohann, P. Keller, H. Runz, S. Köhl, T. Bertsch, K. von Bergmann, et al. 2001. Simvastatin strongly reduces levels of Alzheimer's disease  $\beta$ -amyloid peptides A $\beta$ 42 and A $\beta$ 40 in vitro and in vivo. *Proc. Natl. Acad. Sci. USA*. **98**: 5856–5861.
- Kojro, E., G. Gimple, S. Lammich, W. März, and F. Fahrenholz. 2001. Low cholesterol stimulates the nonamyloidogenic pathway by its effect on the  $\alpha$ -secretase ADAM 10. *Proc. Natl. Acad. Sci. USA*. **98**: 5815–5820.
- Simons, M., P. Keller, B. De Strooper, K. Beyreuther, C. G. Dottie, and K. Simons. 1998. Cholesterol depletion inhibits the generation of  $\beta$ -amyloid in hippocampal neurons. *Proc. Natl. Acad. Sci. USA*. **95**: 6460–6464.
- Bodovitz, S., and W. L. Klein. 1996. Cholesterol modulates  $\alpha$ -secretase cleavage of amyloid precursor protein. *J. Biol. Chem.* **271**: 4436–4440.
- Buxbaum, J. D., N. S. Geoghagan, and L. T. Friedhoff. 2001. Cholesterol depletion with physiological concentrations of a statin decreases the formation of the Alzheimer amyloid Abeta peptide. *J. Alzheimers Dis.* **3**: 221–229.
- Ehehalt, R., P. Keller, C. Haass, C. Thiele, and K. Simons. 2003. Amyloidogenic processing of the Alzheimer  $\beta$ -amyloid precursor protein depends on lipid rafts. *J. Cell Biol.* **160**: 113–123.
- Runz, H., J. Rietdorf, I. Tomic, M. de Bernard, K. Beyreuther, R. Pepperkok, and T. Hartmann. 2002. Inhibition of intracellular cholesterol transport alters presenilin localization and amyloid precursor protein processing in neuronal cells. *J. Neurosci.* **22**: 1679–1699.
- Dean, M., and R. Allikmets. 2001. Complete characterization of the human ABC gene family. *J. Bioenerg. Biomembr.* **33**: 475–479.
- Dean, M., Y. Hamon, and G. Chimini. 2001. The human ATP-binding cassette (ABC) transporter superfamily. *J. Lipid Res.* **42**: 1007–1017.
- Schmitz, G., W. E. Kaminski, and E. Orsó. 2000. ABC transporters in cellular lipid trafficking. *Curr. Opin. Lipidol.* **11**: 493–501.
- Schmitz, G., T. Langmann, and S. Heimerl. 2001. Role of ABCG1 and other ABCG family members in lipid metabolism. *J. Lipid Res.* **42**: 1513–1520.
- Tachikawa, M., M. Watanabe, S. Hori, M. Fukaya, S. Ohtsuki, T. Asashima, and T. Terasaki. 2005. Distinct spatio-temporal expression of ABCA and ABCG transporters in the developing and adult mouse brain. *J. Neurochem.* **95**: 294–304.
- Klucken, J., C. Büchler, E. Orsó, W. E. Kaminski, M. Porsch-Özcürüm, G. Liebisch, M. Kapinsky, W. Diederich, W. Drobnik, M. Dean, et al. 2000. ABCG1 (ABC8), the human homologue of the *Drosophila* white gene, is a regulator of macrophage cholesterol and phospholipid transport. *Proc. Natl. Acad. Sci. USA*. **97**: 817–822.
- Nakamura, K., M. A. Kennedy, A. Baldán, D. D. Bohanic, K. Lyons, and P. A. Edwards. 2004. Expression and regulation of multiple murine ATP-binding cassette transporter G1 mRNAs/isoforms that stimulate cellular cholesterol efflux to high density lipoprotein. *J. Biol. Chem.* **279**: 45980–45989.
- Wang, N., D. Lan, W. Chen, F. Matsuura, and A. R. Tall. 2004. ATP-binding cassette transporters G1 and G4 mediate cellular cholesterol efflux to high-density lipoproteins. *Proc. Natl. Acad. Sci. USA*. **101**: 9774–9779.
- Vaughan, A. M., and J. F. Oram. 2005. ABCG1 redistributes cell cholesterol to domains removable by HDL but not by lipid-depleted apolipoproteins. *J. Biol. Chem.* **280**: 30150–30157.
- Kennedy, M. A., G. C. Barrera, K. Nakamura, A. Baldán, P. Tarr, M. C. Fishbein, J. Frank, O. L. Francone, and P. A. Edwards. 2005. ABCG1 has a critical role in mediating cholesterol efflux to HDL and preventing cellular lipid accumulation. *Cell Metab.* **1**: 121–131.
- Karten, B., R. B. Campenot, D. E. Vance, and J. E. Vance. 2006. Expression of ABCG1, but not ABCA1, correlates with cholesterol release by cerebellar astroglia. *J. Biol. Chem.* **281**: 4049–4057.
- Chen, H., M. D. Rossier, A. Lalioti, A. Lynn, A. Charkravarti, G. Perrin, and S. E. Antonarakis. 1996. Cloning of the cDNA for a human homologue of the *Drosophila* white gene and mapping to chromosome 21q22.3. *Am. J. Hum. Genet.* **59**: 66–75.
- Langmann, T., M. Porsch-Özcürüm, U. Unkelbach, J. Klucken, and G. Schmitz. 2000. Genomic organization and characterization of the promoter of the human ATP-binding cassette transporter-G1 (ABCG1) gene. *Biochim. Biophys. Acta*. **1494**: 175–180.
- Lorkowski, S., S. Rust, T. Engel, E. Jung, K. Tegelkamp, E. A. Galinski, G. Assmann, and P. Cullen. 2001. Genomic sequence and structure of the human ABCG1 (ABC8) gene. *Biochem. Biophys. Res. Commun.* **280**: 121–131.
- Kennedy, M. A., A. Venkateswaran, P. T. Tarr, I. Xenarios, J. Kudoh, N. Shimizu, and P. A. Edwards. 2001. Characterization of the human ABCG1 gene. *J. Biol. Chem.* **276**: 39438–39447.
- Hattori, M., A. Fujiyama, T. D. Taylor, H. Watanabe, T. Yada, H. S. Park, A. Toyoda, K. Ishii, Y. Totoki, D. K. Choi, et al. 2000. The DNA sequence of human chromosome 21. *Nature*. **405**: 311–319.
- McCormick, M., A. Schinzel, M. Petersen, G. Stetten, D. Driscoll, E. Cantu, L. Tranebjaerg, M. Mikkelsen, P. Watkins, and S. Antonarakis. 1989. Molecular genetic approach to the characterization of the Down syndrome region of chromosome 21. *Genomics*. **5**: 325–331.
- Rahmani, Z., J. Blouin, N. Creau-Goldberg, P. Watkins, J. Mattei, M. Poissonnier, M. Prieur, Z. Chettouh, A. Nicole, A. Aurias, et al. 1989. Critical role of D21S55 region on chromosome 21 in the pathogenesis of Down syndrome. *Proc. Natl. Acad. Sci. USA*. **86**: 5958–5962.



33. Korenberg, J. R., H. Kawashima, S. M. Pulst, T. Ikeuchi, N. Ogasawara, K. Yamamoto, S. A. Schonberg, R. West, L. Allen, E. Magenis, et al. 1990. Molecular definition of a region of chromosome 21 that causes features of the Down syndrome phenotype. *Am. J. Hum. Genet.* **47**: 236–246.
34. Korenberg, J. R., X. N. Chen, R. Schipper, Z. Sun, R. Gonsky, S. Gerwehr, N. Carpenter, C. Daumer, P. Dignan, C. Disteché, et al. 1994. Down syndrome phenotypes: the consequences of chromosomal imbalance. *Proc. Natl. Acad. Sci. USA.* **91**: 4997–5001.
35. Lott, I. T., and E. Head. 2001. Down syndrome and Alzheimer's disease: a link between development and aging. *Ment. Retard. Dev. Disabil. Res. Rev.* **7**: 172–178.
36. Epstein, C. J. 2001. Down syndrome. In *The Metabolic and Molecular Bases of Inherited Disease*. C. R. Scriver, A. L. Beaudet, W. S. Sly, and D. Valle, editors. McGraw-Hill, New York. 1223–1256.
37. Wisniewski, H., J. Wegiel, and E. Popovitch. 1995. Age-associated development of diffuse and thioflavin-S-positive plaques in Down syndrome. *Dev. Brain Dysfunct.* **7**: 330–339.
38. Prasher, V. P. 1995. Prevalence of psychiatric disorders in adults with Down syndrome. *Eur. J. Psychiatry.* **9**: 77–82.
39. Prasher, V. P., M. J. Farrer, A. M. Kessling, E. M. Fisher, R. J. West, P. C. Barber, and A. C. Butler. 1998. Molecular mapping of Alzheimer-type dementia in Down's syndrome. *Ann. Neurol.* **43**: 380–383.
40. Rovelet-Lecrux, A., D. Hannequin, G. Raux, N. Le Meur, A. Laquerrière, A. Vital, C. Dumanchin, S. Fueilleux, A. Brice, M. Vercelletto, et al. 2006. APP locus duplication causes autosomal dominant early-onset Alzheimer's disease with cerebral amyloid angiopathy. *Nat. Genet.* **38**: 24–26.
41. Myers, A., F. Wavrant-De Vrieze, P. Holmans, M. Hamshere, R. Crook, D. Compton, H. Marshall, D. Meyer, S. Shears, J. Booth, et al. 2002. Full genome search for Alzheimer's disease: stage II analysis. *Am. J. Med. Genet.* **114**: 235–244.
42. Wellington, C. L., Y.-Z. Yang, S. Zhou, S. M. Clee, B. Tan, K. Hirano, K. Zwarts, A. Kwok, A. Gelfer, M. Marcil, et al. 2002. Truncation mutations in ABCA1 suppress normal upregulation of full-length ABCA1 by 9-cis-retinoic acid and 22-R-hydroxycholesterol. *J. Lipid Res.* **43**: 1939–1949.
43. Albrecht, C., S. Soumian, J. S. Amey, A. Sardini, C. F. Higgins, A. H. Davies, and R. G. Gibbs. 2004. ABCA1 expression in carotid atherosclerotic plaques. *Stroke.* **35**: 2801–2806.
44. Wang, N., M. Ranalletta, F. Matsuura, F. Peng, and A. Tall. 2006. LXR-induced redistribution of ABCG1 to plasma membrane in macrophages enhances cholesterol mass efflux to HDL. *Arterioscler. Thromb. Vasc. Biol.* **26**: 1310–1316.
45. Li, Y., M. Ge, L. Ciani, G. Kuriakose, E. J. Westover, M. Dura, D. F. Covey, J. H. Freed, F. R. Maxfield, J. Lytton, et al. 2004. Enrichment of endoplasmic reticulum with cholesterol inhibits sarcoplasmic-endoplasmic reticulum calcium ATPase-2b activity in parallel with increased order of membrane lipids. *J. Biol. Chem.* **279**: 37030–37039.
46. DeMattos, R. B., M. A. O'Dell, M. Parsadanian, J. W. Taylor, J. A. K. Harmony, K. R. Bales, S. M. Paul, B. J. Aronow, and D. M. Holtzman. 2002. Clusterin promotes amyloid plaque formation and is critical for neurotoxicity in a mouse model of Alzheimer's disease. *Proc. Natl. Acad. Sci. USA.* **99**: 10843–10848.
47. Chyung, J. H., and D. J. Selkoe. 2003. Inhibition of receptor-mediated endocytosis demonstrates generation of amyloid  $\beta$ -protein at the cell surface. *J. Biol. Chem.* **278**: 51035–51043.
48. Chyung, J. H., D. M. Raper, and D. J. Selkoe. 2005.  $\gamma$ -Secretase exists on the plasma membrane as an intact complex that accepts substrates and effects intramembrane cleavage. *J. Biol. Chem.* **280**: 4383–4392.
49. Kaether, C., S. Schmitt, M. Willen, and C. Haass. 2006. Amyloid precursor protein and notch intracellular domains are generated after transport of their precursors to the cell surface. *Traffic.* **7**: 408–415.
50. Kinoshita, A., H. Fukumoto, T. Shah, C. M. Whelan, M. C. Irizarry, and B. T. Hyman. 2003. Demonstration by FRET of BACE interaction with the amyloid precursor protein at the cell surface and in early endosomes. *J. Cell Sci.* **116**: 3339–3346.
51. Pasternak, S. H., R. D. Bagshaw, M. Guiral, S. Zhang, C. A. Ackerley, C. Callahan, and D. J. Mahuran. 2003. Presenilin-1, nicastrin, APP and gamma-secretase activity are co-localized in the lysosomal membrane. *J. Biol. Chem.* **278**: 26687–26694.
52. Riddell, D. R., G. Christie, I. Hussain, and C. Dingwall. 2001. Compartmentalization of  $\beta$ -secretase (Asp2) into low-buoyant density, noncaveolar lipid rafts. *Curr. Biol.* **11**: 1288–1293.
53. Vetrivel, K. S., H. Cheng, S. H. Kim, Y. Chen, N. Y. Barnes, A. T. Parent, S. S. Sisodia, and G. Thinakaran. 2005. Spatial segregation of  $\gamma$ -secretase and substrates in distinct membrane domains. *J. Biol. Chem.* **280**: 25892–25900.
54. Hayden, M. R., S. M. Clee, A. Brooks-Wilson, J. Genest, Jr., A. Attie, and J. J. P. Kastelein. 2000. Cholesterol efflux regulatory protein, Tangier disease and familial high-density lipoprotein deficiency. *Curr. Opin. Lipidol.* **11**: 117–122.
55. Rust, S., M. Rosier, H. Funke, Z. Amoura, J.-C. Piette, J.-F. Deleuze, H. B. Brewer, Jr., N. Duverger, P. Denéfle, and G. Assmann. 1999. Tangier disease is caused by mutations in the gene encoding ATP-binding cassette transporter 1. *Nat. Genet.* **22**: 352–355.
56. Brooks-Wilson, A., M. Marcil, S. M. Clee, L. Zhang, K. Roomp, M. van Dam, L. Yu, C. Brewer, J. A. Collins, H. O. F. Molhuizen, et al. 1999. Mutations in ABC1 in Tangier disease and familial high-density lipoprotein deficiency. *Nat. Genet.* **22**: 336–345.
57. Bodzioch, M., E. Ors6, J. Klucken, T. Langmann, A. Böttcher, W. Diederich, W. Drobnik, S. Barlage, C. Büchler, M. Porsch-Özcürüm, et al. 1999. The gene encoding ATP-binding cassette transporter 1 is mutated in Tangier disease. *Nat. Genet.* **22**: 347–351.
58. Fukumoto, H., A. Deng, M. C. Irizarry, M. L. Fitzgerald, and G. W. Rebeck. 2002. Induction of the cholesterol transporter ABCA1 in CNS cells by LXR agonists increases secreted A $\beta$  levels. *J. Biol. Chem.* **277**: 48508–48513.
59. Koldamova, R. P., I. M. Lefterov, M. D. Ikonovic, J. Skoko, P. I. Lefterov, B. A. Isanski, S. T. DeKosky, and J. S. Lazo. 2003. 22R-Hydroxycholesterol and 9-cis-retinoic acid induce ATP-binding cassette transporter A1 expression and cholesterol efflux in brain cells and decrease amyloid  $\beta$  secretion. *J. Biol. Chem.* **278**: 13244–13256.
60. Sun, Y., J. Yao, T.-W. Kim, and A. R. Tall. 2003. Expression of LXR target genes decreases cellular amyloid  $\beta$  peptide secretion. *J. Biol. Chem.* **278**: 27688–27694.
61. Hirsch-Reinshagen, V., L. F. Maia, B. L. Burgess, J. F. Blain, K. E. Naus, S. A. McIsaac, P. F. Parkinson, J. Y. Chan, G. H. Tansley, M. R. Hayden, et al. 2005. The absence of ABCA1 decreases soluble apoE levels but does not diminish amyloid deposition in two murine models of Alzheimer's disease. *J. Biol. Chem.* **280**: 43243–43256.
62. Wahrle, S., H. Jiang, M. Parsadanian, R. E. Hartman, K. R. Bales, S. M. Paul, and D. M. Holtzman. 2005. Deletion of Abca1 increases Abeta deposition in the PDAPP transgenic mouse model of Alzheimer disease. *J. Biol. Chem.* **280**: 43236–43242.
63. Koldamova, R., M. Staufenbiel, and I. Lefterov. 2005. Lack of ABCA1 considerably decreases brain apoE level and increases amyloid deposition in APP23 mice. *J. Biol. Chem.* **280**: 43224–43235.
64. Burns, M. P., L. Vardanian, A. Pajoohesh-Gangi, L. Wang, M. Cooper, D. C. Harris, K. Duff, and G. W. Rebeck. 2006. The effects of ABCA1 on cholesterol efflux and A $\beta$  levels in vitro and in vivo. *J. Neurochem.* **98**: 792–800.
65. Hirsch-Reinshagen, V., S. Zhou, B. L. Burgess, L. Bernier, S. A. McIsaac, J. Y. Chan, G. H. Tansley, J. S. Cohn, M. R. Hayden, and C. L. Wellington. 2004. Deficiency of ABCA1 impairs apolipoprotein E metabolism in brain. *J. Biol. Chem.* **279**: 41197–41207.
66. Wahrle, S. E., H. Jiang, M. Parsadanian, J. Legleiter, X. Han, J. D. Fryer, T. Kowalewski, and D. M. Holtzman. 2004. ABCA1 is required for normal CNS apoE levels and for lipidation of astrocyte-secreted apoE. *J. Biol. Chem.* **279**: 40987–40993.
67. Kim, W. S., A. S. Rahmanto, A. Kamili, K. A. Rye, G. J. Guillemin, I. C. Gelissen, W. Jessup, A. F. Hill, and B. Garner. 2007. Role of ABCG1 and ABCA1 in regulation of neuronal cholesterol efflux to apolipoprotein E discs and suppression of amyloid- $\beta$  peptide generation. *J. Biol. Chem.* **282**: 2851–2861.
68. Sun, X., Y. Tong, H. Qing, C.-H. Chen, and W. Song. 2006. Increased BACE1 maturation contributes to the pathogenesis of Alzheimer's disease in Down syndrome. *FASEB J.* **20**: 1361–1368.
69. Nistor, M., M. Don, M. Parekh, F. Sarsoza, M. Goodus, G. E. Lopez, C. Kawas, J. Leverenz, E. Doran, I. T. Lott, et al. 2006. Alpha- and beta-secretase activity as a function of age and beta-amyloid in Down syndrome and normal brain. *Neurobiol. Aging.* In press.
70. Sun, X., G. He, and W. Song. 2006. BACE2, as a novel APP theta-secretase, is not responsible for the pathogenesis of Alzheimer's disease in Down syndrome. *FASEB J.* **20**: 1369–1376.
71. Tanzi, R. E., A. I. McClatchey, E. D. Lamperti, L. Villa-Komaroff, J. F. Gusella, and R. L. Neve. 1988. Protease inhibitor domain encoded by an amyloid protein precursor mRNA associated with Alzheimer's disease. *Nature.* **331**: 528–530.

72. Oyama, F., N. J. Cairns, H. Shimada, R. Oyama, K. Titani, and Y. Ihara. 1994. Down's syndrome: up-regulation of  $\beta$ -amyloid protein precursor and  $\tau$  mRNAs and their defective coordination. *J. Neurochem.* **62**: 1062–1066.
73. Mao, R., C. L. Zielke, H. R. Zielke, and J. Pevsner. 2003. Global up-regulation of chromosome 21 gene expression in the developing Down syndrome brain. *Genomics.* **81**: 457–467.
74. Engidawork, E., N. Baiic, M. Fountoulakis, M. Dierssen, S. Greber-Platzer, and G. Lubec. 2001. Beta-amyloid precursor protein, ETS-2 and collagen alpha 1 (VI) chain precursor, encoded on chromosome 21, are not overexpressed in fetal Down syndrome: further evidence against gene dosage effect. *J. Neural Transm. Suppl.* **61**: 335–346.
75. Griffin, W. S. T., J. G. Sheng, J. E. McKenzie, M. C. Royston, S. M. Gentleman, R. A. Brumback, L. C. Cork, M. R. Del Bigio, G. W. Roberts, and R. E. Mrak. 1998. Life-long overexpression of S100 $\beta$  in Down's syndrome: implications for Alzheimer pathogenesis. *Neurobiol. Aging.* **19**: 401–405.
76. Argellati, F., S. Massone, C. d'Abramo, U. M. Marinari, M. A. Pronzato, C. Domenicotti, and R. Ricciarelli. 2006. Evidence against the overexpression of APP in Down syndrome. *IUBMB Life.* **58**: 103–106.
77. Deutsch, S., R. Lyle, E. T. Dermitzakis, H. Attar, L. Subrahmanyam, C. Gehrig, L. Parand, M. Gagnebin, J. Rougemont, C. V. Jongeneel, et al. 2005. Gene expression variation and expression quantitative trait mapping of human chromosome 21 genes. *Hum. Mol. Genet.* **14**: 3741–3749.
78. Fitzpatrick, D. R., J. Ramsay, N. I. McGill, M. Shade, A. D. Carothers, and N. D. Hastie. 2002. Transcriptome analysis of human autosomal trisomy. *Hum. Mol. Genet.* **11**: 3249–3256.